Cellulose (2023) 30:413–426
https://doi.org/10.1007/s10570-022-04889-9

ORIGINAL RESEARCH

Cellulose acetate/polyvinylidene fluoride based mixed matrix membranes impregnated with UiO-66 nano-MOF for reverse osmosis desalination

Omneya A. Koriem · Marwa S. Showman · Ahmed H. El-Shazly · Marwa F. Elkady

Received: 23 March 2022 / Accepted: 8 October 2022 / Published online: 2 November 2022

Abstract Reverse osmosis (RO) is considered a lifesaver technology to conquer the current catastrophic water shortage situation. However, reaching a competitive RO membrane is a challenging issue. Therefore, this study investigated the optimum polymeric blending ratio between cellulose acetate (CA) and polyvinylidene fluoride (PVDF) to have a new blended polymeric membrane named cellulose acetate polyvinyl (CAPV-X), where X is the PVDF concentration %, with enhanced properties. The optimum prepared CA/PVDF blended membrane was selected for further enhancement with nano sized metal organic framework (UiO-66 MOF). Selection was made depending on each membrane salt rejection. A membrane characterization was performed based on Fourier transform infrared (FTIR), X-ray diffractometer (XRD), scanning electron microscope, thermal gravimetric analysis, and contact angle. FTIR and XRD data confirmed the successful preparation of the blended polymeric membranes CAPV-5, CAPV-7 and CAPV-10. Further, they proved UiO-66 nanofiller impregnation in the hybrid CA/PVDF/UiO-66 membrane (CPU). The addition of PVDF and nano-MOF had a slight positive effect on the membrane thermal stability. The contact angle increased with increasing the PVDF concentration and decreased once more with the impregnation of UiO-66. The RO membrane performance revealed that the optimum CA/PVDF ratio was found to be 93/7% with around 80% salt rejection and a permeate water flux of 4 L/m^2 h. CPU composite membrane was then fabricated to enhance salt rejection and permeate water flux. The testing data indicated that salt rejection and permeate water flux increased over blended CAPV-7 membrane by almost 12% and 42%, respectively. Overall, CPU hybrid membrane could be used for water desalination with a good salt rejection of 90.2% and a permeate water flux of 5.7 L/m^2 h.

O. A. Koriem (✉) · A. H. El-Shazly · M. F. Elkady
Chemical and Petrochemicals Engineering Department, Egypt-Japan University of Science and Technology (E-JUST), Alexandria 21934, Egypt
e-mail: omneya.koriem@ejust.edu.eg

M. S. Showman · M. F. Elkady
Fabrication Technology Department, Advanced Technology and New Materials Research Institute (ATNMRI), The City of Scientific Research and Technological Applications (SRTA-City), Alexandria, Egypt

A. H. El-Shazly
Chemical Engineering Department, Faculty of Engineering, Alexandria University, Alexandria 21544, Egypt

Graphical abstract

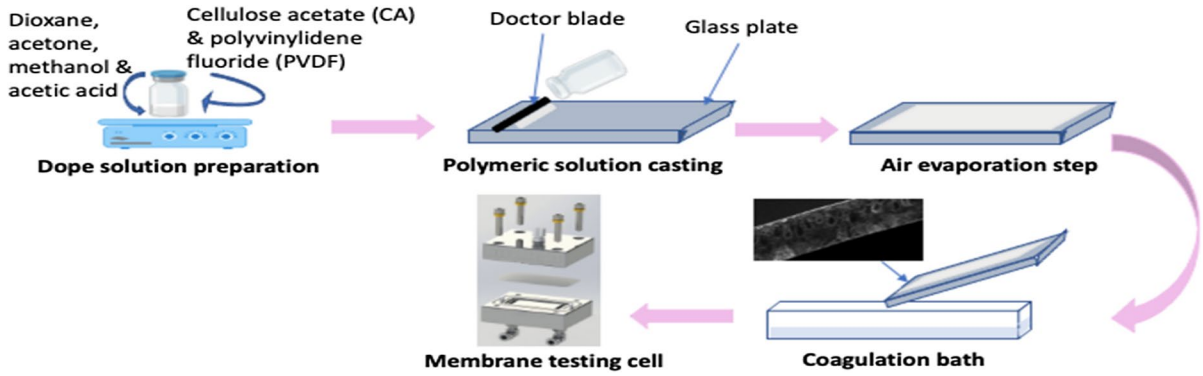

Keywords Cellulose acetate · Asymmetric membrane · Mixed matrix membrane · Desalination · Reverse osmosis · UiO-66

Introduction

Undoubtedly, water is the most vital and precious element on Earth. It is nature's gift and without it, almost no human survival activity would be achievable. Thus, battles and conflicts over accessing fresh, clean, and permanent water resources have been taking place since an immemorial time (Salameh et al. 2021). Climate change, growth of population, and contamination by industrialization made the water problem even worse. Consequently, countries have searched for alternative solutions to overcome the water shortage crisis. Desalination has played a key effective role in diminishing the gap between the desired amount of fresh water and the available resources. In 2020, It was reported that around 97.2 million m^3/day of fresh water is supplied by desalination plants. Amongst the available desalination techniques, reverse osmosis (RO) is dominating the world market, where it accounts for 85% of the already existing plants (Zhao et al. 2021). RO is a membrane-based technology that is characterized over thermal desalination by its flexible processing, cost efficiency, and low energy requirement. Various parameters affect the performance of RO units including the selection of the right membrane material and its synthesizing method, the type of membrane module, and operating parameters (El-Gendi et al. 2017).

For many years, cellulose acetate (CA) asymmetric and polyamide thin film composite (TFC) have been the two dominant types of RO membranes. Even though polyamide-TFC membranes showed many pros over CA membranes, namely, high water permeation flux and better salt rejection, the desalination market still relies on CA membranes for their stable performance, durability, relatively low cost, simple processing, and tolerance to free chlorine attack. However, producing CA membranes with enhanced mechanical and thermal stability, salt rejection as well as water permeation flux is a priority to compete and cope with the development of TFC membranes and this may eventually affect the RO market in the near future (Ghaseminezhad et al. 2019; Liu et al. 2019b; Abdelhamid and Khalil 2019; Ali et al. 2021). Accordingly, membranologists have investigated two membrane modification approaches to overcome the disadvantages of polymeric membranes. The bulk membrane modification, such as the usage of multiple polymeric blends and impregnation of organic or inorganic particles. The other approach is by enhancing the membrane surface, for instance, grafting hydrophilic monomers to the membrane surface or introducing polar groups to alter the membrane chemical structure (El-Ghaffar et al. 2020; Elessawy et al. 2020; Elkady et al. 2020; Elkony et al. 2020; Batool et al. 2021).

The most common approaches for water treatment are blending two polymers and incorporating solid materials within the polymer matrix, or as called mixed matrix membranes (MMMs). Those approaches aim to obtain a new membrane with hybrid characteristics between those of its blended and/or incorporated components (Sivakumar et al.

2006; El-Aassar et al. 2016; Siddique et al. 2021). According to literature, the synthesis of blended polymers, with a selectivity better than the base polymer, is driven by the need to superimpose certain characteristics over those of the homopolymer. Accordingly, the properties, as well as the balance of the hydrophilic- hydrophobic membrane system, can be controlled when blending multi polymeric components(Nagendran et al. 2008; Arthanareeswaran and Kumar 2010; Moradihamedani and Abdullah 2017). Polyvinylidene fluoride (PVDF) is a polymeric membrane material that is strongly fabricated by phase inversion method and used in water treatment purposes for its chemical, thermal and incredible mechanical stability (Haponska et al. 2017; Lu et al. 2021; Shah et al. 2021). As previously stated in the literature, PVDF/CA blend membrane was prepared via phase inversion technique only in a few studies, where PVDF was the dominant polymer and CA was blended with minor concentration. The aim of CA addition was either for its hydrophilic properties to be applied at different applications rather than RO, such as sewage filtration (Hossein Razzaghi et al. 2014), juice clarification (Fitri and Widiastuti 2017), membrane bioreactor (Razzaghi et al. 2018) and ultrafiltration (Reza et al. 2022), or for its good conductivity to be used in lithium batteries (Cui et al. 2017). However, the blending of CA as a major matrix with PVDF to fabricate a completely hydrophilic membrane with suitable mechanical properties for RO application is considered the first investigation. On the other hand, metal–organic frameworks (MOFs) have attracted the attention in various applications for their marvelous properties. Amongst the prepared MOFs, UiO-66 as a hydrophilic filler was studied by many researchers for water desalination. It is known for its huge surface area and stability in different and harsh conditions (Kadhom et al. 2017).

As far as the authors know, there is no other research that deals with the fabrication of CA/PVDF blended polymeric membrane that is hybridized with UiO-66 nano MOF for RO application. Accordingly, this investigation seeks to boost CA performance by blending it with polymeric PVDF to obtain CA/PVDF blended RO membrane via phase inversion. In addition, the effect of impregnating UiO-66 nanoparticles on enhancing the RO performance of the new blended CA/PVDF polymeric membrane was investigated. The characteristics of the resultant hybrid polymeric membranes were tested by FTIR, XRD, TGA, SEM, and contact angle. Moreover, their RO performance including permeation and salt rejection will be discussed.

Experimental work

Materials

All chemicals, except sodium chloride (NaCl), were of analytical grade and used with no further purification or modification. Cellulose acetate (CA) with 100,000 g/mol average molecular weight and 39.8% acetyl content was supplied by Acros Organics, Polyvinylidene fluoride (PVDF) was obtained from Alfa Aesar. 1,4-dioxane (≥ 99.8%) and acetone (≥ 99.8%) were purchased from Fisher, methanol ($CH_3OH \geq 99.8\%$) was delivered by Sigma Aldrich and acetic acid (glacial) was provided by Merck.

Fabrication of blank CA, blended CA/PVDF and CA/PVDF/UiO-66 hybrid membranes

Phase inversion method was used to obtain all flat sheet membranes under investigation. CA/PVDF blended membranes (CAPV-) were fabricated by preparing two separately homogeneous solutions of CA and PVDF then blending them overnight at 80 °C to avoid the formation of cloudy gel-like viscous solution(Li et al. 2013). Acetone was used as a common solvent for both PVDF and CA polymers. Moreover, dioxane was added as a solvent for the base CA polymer. The addition of acetic acid aimed to enhance the polymer mobility and structure. Methanol behaved as a non-solvent to stimulate the membrane water absorption and accordingly increase the membrane flow performance(Duarte et al. 2006; Abdellah Ali et al. 2020).For CA/PVDF blended polymeric membrane preparation, various amounts of CA were dissolved in a mixture of (dioxane/ acetone/ acetic acid/ methanol) with a ratio of (5.4/2/1/1.6), respectively. While certain amounts of PVDF were dissolved in a mixture of acetone and dioxane (2:1), sequentially. Eventually, the total polymer concentration in the homogeneous blended solution was kept at 14 wt% with the composition as indicated in Table 1. The increase of PVDF composition in the doping polymeric solution above 10 wt% of the polymer

Table 1 Composition and preparation conditions of the obtained membranes

Membrane name	Polymers composition			Phase inversion conditions			
	CA (%)	PVDF (%)	UiO-66 (%)	Water bath temperature	Evaporation time	Annealing temperature	Annealing time
CAPV-0	100	0	0	25 ± 2 °C	30 s	80–85°	10 min
CAPV-5	95	5	0				
CAPV-7	93	7	0				
CAPV-10	90	10	0				
CPU	93	7	0.2				

concentration resulted in a viscous solution that is hard to be casted. For this reason, the maximum blend polymer composition was chosen to be 9:1 of CA to PVDF, respectively. Later, 0.2 wt%, in respect to the weight of total blended polymers, of previously prepared UiO-66 nanoparticles(Koriem et al. 2021) were dispersed in the optimum mixed solvents for 2 h, then the optimum amounts of CA powder and PVDF solution were added to obtain CA/PVDF/UiO-66 (CPU) mixed matrix doping solution. The nanofiller was added to study its effect on the performance of the blended CA/PVDF membrane. The investigated amount of UiO-66 was selected as close to the best performance results obtained from literature (He et al. 2017; Kadhom et al. 2017).

In order to obtain a membrane free from deficiencies caused by air bubbles, the prepared solutions were left before casting for 24 h. Then, blended polymeric solutions were casted on a glass plate at a thickness of 250 µm using an automatic film applicator with a speed of 50 mm/sec. The resultant casted films were left in the air to evaporate before immersing in a distilled water bath, where the solvent/non-solvent exchange took place. The resulted membranes were annealed in a hot water bath. Finally, the annealed membranes were kept for 24 h in distilled water before conducting the RO performance tests.

Physicochemical characterization of blank CA, blended CA/PVDF and CA/PVDF/UiO-66 hybrid membranes

The obtained pristine CA, blended CA/PVDF and CA/PVDF/UiO-66 mixed matrix membranes were dried prior to characterization in a vacuum oven at 60 °C. Images of platinum coated top, bottom, as well as cross section of the membranes were taken using a JEOL JSM-6010 LV- SEMdevice to investigate their morphological characteristics. Bruker Vertex 70- FTIR equipmentwas used to identify and confirm the chemical structure of the fabricated membranes in a wave number range of 400–4000 cm^{-1}. XRD was used to understand the crystalline nature of the fabricated membranes using a Shimadzu XRD-6100 device. TGA was used to understand the thermal stability of the prepared CA based membranes. In (TGA Q50) device, the temperature raised from 0° to 700 °C with a 10 °C/min raising step. The membrane hydrophilicity/hydrophobicity was measured using a contact angle measuring system (DSA 100, KRÜSS). Five random locations, on the surface of each sample, were selected to measure the contact angle to minimize the possible experimental measurement errors. The tensile strength of the pristine, blended and mixed matrix CA-based membranes was measured using a tensile testing device (4468, Instron). The membranes were cut into 10 × 50 mm and tested with an elongation rate of 3 mm/min.

Blank CA, blended CA/PVDF and CA/PVDF/UiO-66 hybrid membranesperformance Evaluation

- In this investigation, the performance of the various prepared membranes was monitored via a CF042 crossflow membrane testing system (Sterlitech, USA). A schematic diagram of RO testing process can be seen in Fig. 1. Membranes were divided into rectangular shapes of 42 cm^2 similarly to the cell active area. A 5000 ppm NaCl solution was prepared and fed to the system from a tank connected to a Hydra-cell high pressure pump at room temperature (25 ± 2 °C) by. The pressure was raised gradually until permeate water

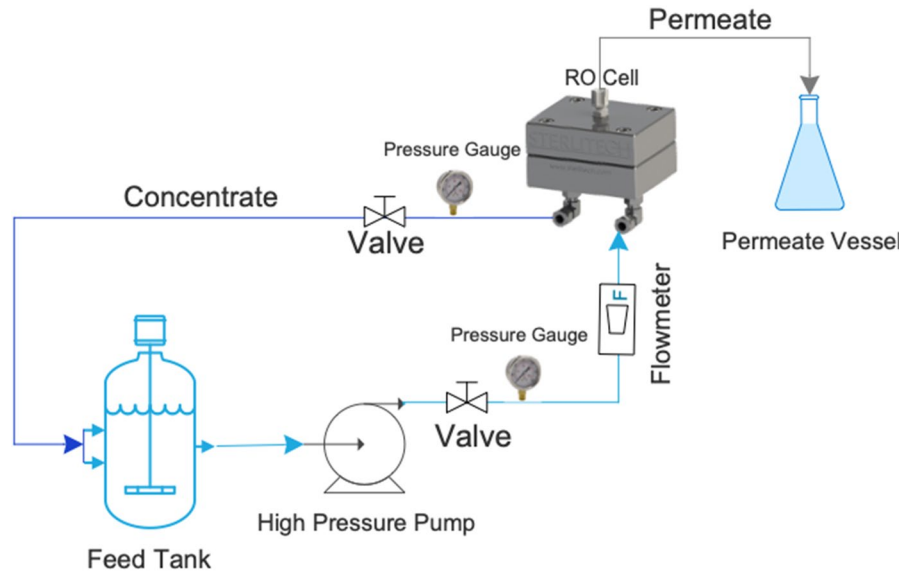

Fig. 1 Schematic diagram of RO membrane testing system

was observed. A sample from the permeate as well as the feedwater was collected, and the concentration of solute was measured by a TDS-meter (Adwa, AD32).Performance evaluation was made based on the permeate water flux and membrane salt rejection calculations as shown in Eqs. (1 and 2)(Ahmad et al. 2015; Ounifi et al. 2021).

$$J = \frac{Q}{A * t} \tag{1}$$

where J is the permeate water flux (L/m2h), Q is the volume of permeate water (L), A is the active are of each membrane (m2), and t is the time (h).

$$R(\%) = 1 - \frac{C_p}{C_i} \tag{2}$$

where R is the membrane salt rejection, Cp and Ci are the permeate and initial feedwater concentration, respectively.

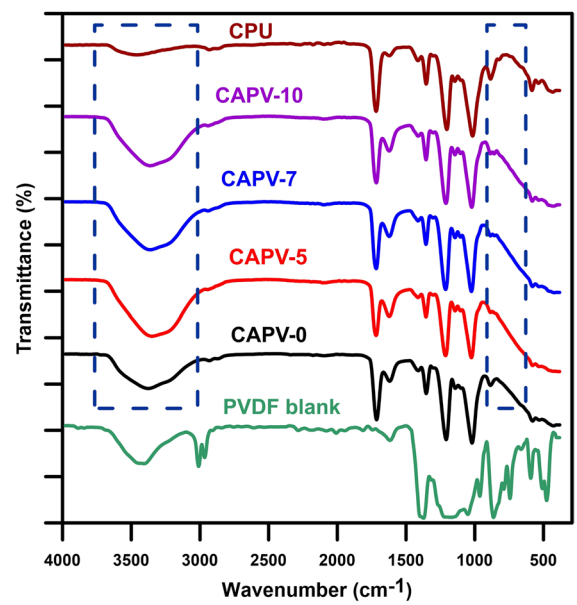

Fig. 2 FTIR spectra of blank PVDF, CA, blended CA/PVDF and hybrid CA/PVDF/UiO-66 membranes

Results and discussion

Blank CA, blended CA/PVDF and CA/PVDF/UiO-66 hybrid membranes Characteristics

- ***FTIR*** analysis was used to identify the characteristic functional groups of the obtained CA membrane as well as, membranes fabricated by blending CA with PVDF with 5, 7 and 10 wt.%. As it can be seen in Fig. 2, the FTIR spectra of pure CA membrane indicated the carboxylic C–O, C–H bond of CH_3, C=O, C–H stretching of CH_2 and OH functional groups at 1036, 1370, 1731, 2949 and 3395 cm^{-1}, respectively.

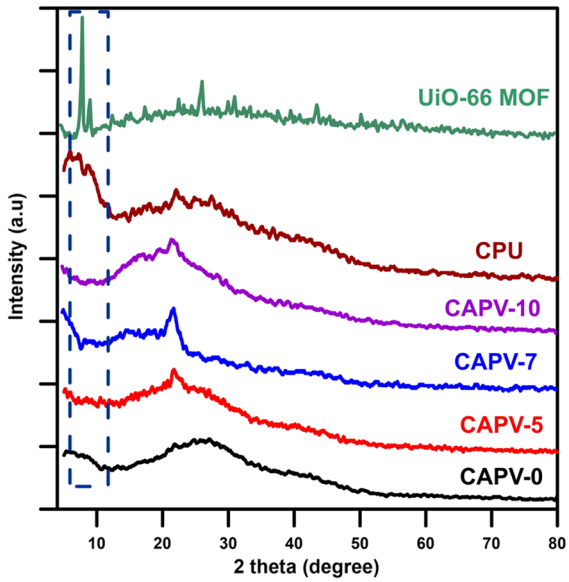

Fig. 3 XRD patterns of UiO-66 nanoparticles, blank CA, blended CA/PVDF and hybrid CA/PVDF/UiO-66 membranes

Close results were previously reported (Liu and Bai 2005; Kamal et al. 2014; Aldalbahi et al. 2020). IR spectra of blended CAPV-5, CAPV-7 and CAPV-10 also showed bands corresponding to the main functional groups of CA. However, a slight shift in band 1036 cm^{-1} and the appearance of new peak at 874 cm^{-1} was observed after the blending of PVDF. This change could be attributed to the PVDF characterized C–C band stretching in β phase and amorphous phase band, respectively(Kang et al. 2016).

The previous observation gave an indication that there was no molecular interaction between PVDF and CA in the blended membranes. Further, after the impregnation of UiO-66 nanoparticles with CA/PVDF blended polymers, a more intense peak at 554 cm^{-1} was formed which could be assigned to the Zr-(OC) stretch (Zhang et al. 2019). These results confirm the interaction between UiO-66 MOF molecules and the hybrid CA/PVDF blending polymer. Additionally, as illustrated and marked in Fig. 2, the peak at 3382 cm^{-1}, which was previously explained as the presence of OH group at CA polymeric matrix, has shifted to 3474 $cm^{-1}$and its intensity decreased significantly after the addition of UiO-66 nanoparticles. This could refer to the interaction between the characterizing carboxylic group of UiO-66 and the present OH group of CA/PVDF blending via hydrogen bond (Sharma et al. 2018). In return, this could give an indication of the physical interaction between UiO-66 nanoparticles and CA/PVDF blended polymers. In conclusion, the previous observations indicated the presence of UiO-66 NPs in the prepared CPU membrane.

XRD crystographic identification was chosen to investigate the effect of PVDF addition on the crystalline nature of pure CA membrane. Further, the presence of UiO-66 nanoparticles was proven by XRD patterns. The amorphous nature of pure CA membrane was clearly illustrated in Fig. 3, its characteristic peaks are relatively wide peaks at 2θ in the regions around 10° and 22° (Xu et al. 2016; Silva et al. 2017). In addition, a strong peak appeared at 21° after the PVDF addition and this could be attributed to the PVDF characteristic β phase(Ahmed et al. 2021). Furthermore, the successful impregnation of UiO-66 nanoparticles into CA/PVDF polymeric blended membrane was proved by the appearance of sharp characteristic peaks of UiO-66 in CPU membrane at 2θ = 7.5° and 8.6° (Schelling et al. 2018).

SEM micrographs were used to investigate the morphological effect of polymeric PVDF blending with neat CA and UiO-66 nanoparticles impregnation on the blank CA membrane. Generally, the phase inversion fabricated anisotropic (asymmetric) CA membranes consist of a thin layer at the top that formed during the solvent evaporation step. This layer is followed by a thick, porous layer formed during the solvent/nonsolvent exchange. The thin layer is responsible for controlling both permeate water flux and salt rejection process, while the porous sublayer layer provided the required mechanical stability. (Strathmann et al. 1971; Suzana Pereira Nunes and Klaus-Viktor Peinemann 2006; Hołda and Vankelecom 2015; Ning 2015; Rana et al. 2015; Werber et al. 2017).

It is illustrated from the cross-section images in Figs. 4c, 5c, and 6c) that all the fabricated CA-based membranes are composed of a dense top layer supported on a sponge-like porous layer, which agrees with the expected design investigated in the literature.

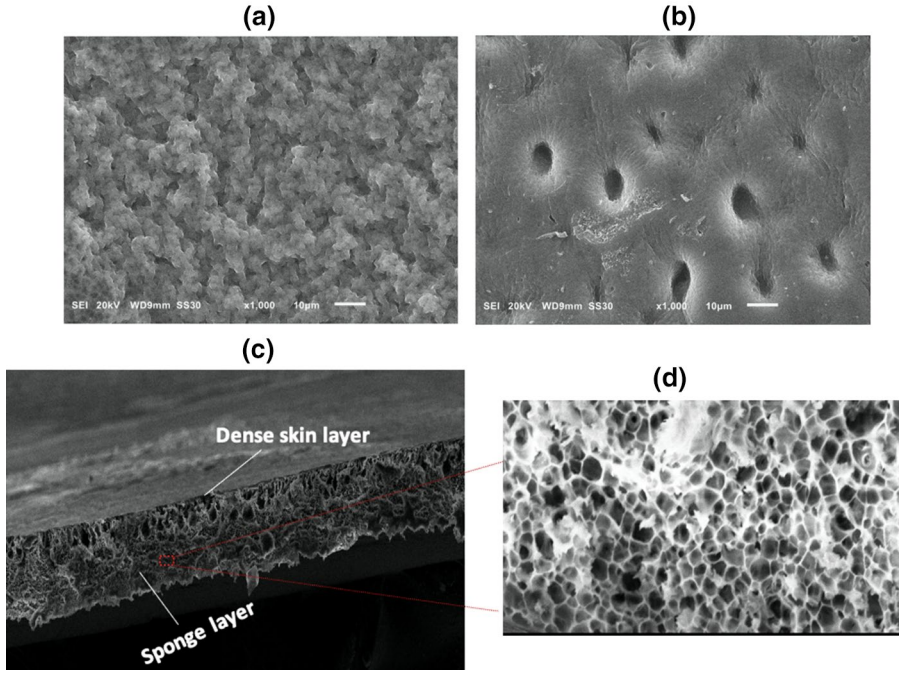

Fig. 4 SEM Images of neat CA membrane **a** top **b** bottom **c** cross section and **d** sponge layer

Figure 4 displays top, bottom, and cross-section surfaces of pristine CA. As shown in Fig. 4c, the surface of the pristine CA membrane has a dense, groovy, and thin top selective layer, that is supported on a thick, porous sublayer. The sublayer is characterized by a tear or finger like structure supported on a sponge like pore structure(Elkony et al. 2020; Ali et al. 2021).As shown in Fig. 4b, the bottom surface of the pristine membrane contains pinholes as a result to the solvent-nonsolvent exchange across the interface(Morsy et al. 2016).

The change in the morphological structure of the pristine CA membrane with the addition of different amounts of PVDF is demonstrated in Fig. 5. Interestingly as illustrated in Fig. 5a, with increasing the PVDF concentration, the corrugated shape of the pristine CA membrane became smoother and the shape of the ridges and grooves on the surface decreased. Nevertheless, large agglomerations are detected on the surface of CAPV-10 membrane, which might cause defects in the membrane performance. Additionally, comparing to neat CA membrane, it was noticed from Fig. 5b that the number of pores was increased in the bottom surface. Moreover, in comparison to CAPV-0, it was found that the addition of PVDF resulted in a small increase in the selective dense top layer. This might explain the membrane's enhanced salt rejection and the membrane's decreased permeate water flux. However, as displayed in Fig. 5c, the thickness of the supportive sponge layer increase with increasing the amount of PVDF added. This might be explained by the delay of the demixing process during the membrane solidification in the coagulation bath (Ghaffarian et al. 2013; Struzyńska-Piron et al. 2014). Despite that, the blending of PVDF with CA does not have a noticeable change on the total membrane thickness, where all fabricated membranes thickness were found to be 85 ± 15 µm.

On the other side, the hydrophilic UiO-66 impregnation influenced the pore structure of the membrane. The presence of hydrophilic UiO-66 NPs in the dope solution increased the exchange rate of solvent and non-solvent. This led to a more uniform and increased number of a longer finger-like on a spongeous pore structure as well as a porous structure of the bottom surface, this can be seen in Fig. 6c and Fig. 6b, respectively. In addition, a thicker top selective layer than CAPV-7 was observed in Fig. 6c. The selective layer is responsible for the rejection and causes a resistance to the permeate water flux. Nevertheless, due to the high hydrophilic nature of UiO-66, the permeate water flux was enhanced. Also, white particles can be seen in Fig. 6a on the top surface of the membrane, and this is attributed to the successful

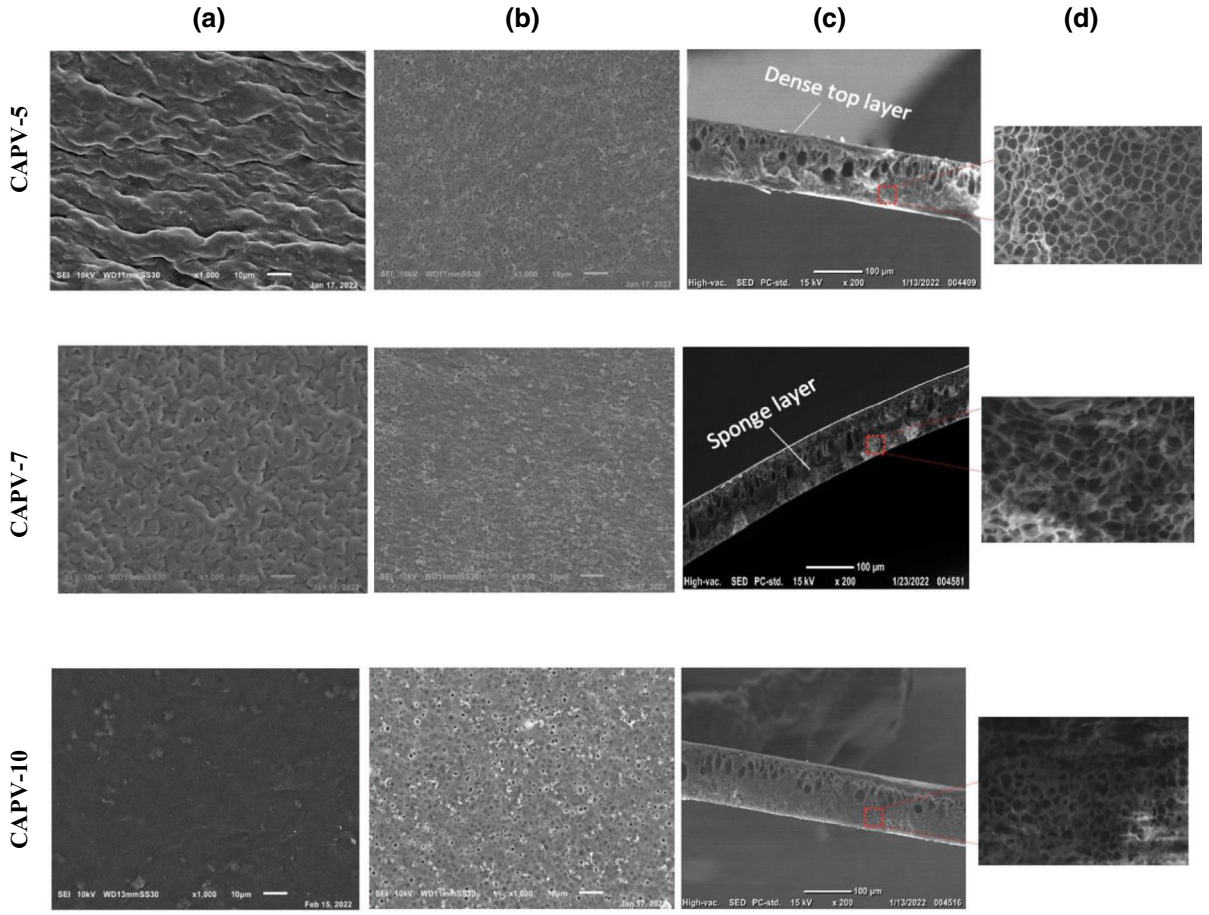

Fig. 5 SEM Images of **a** top **b** bottom and **c** cross section **d** sponge layer of the synthesized CAPV-5, CAPV-7 and CAPV-10 membranes

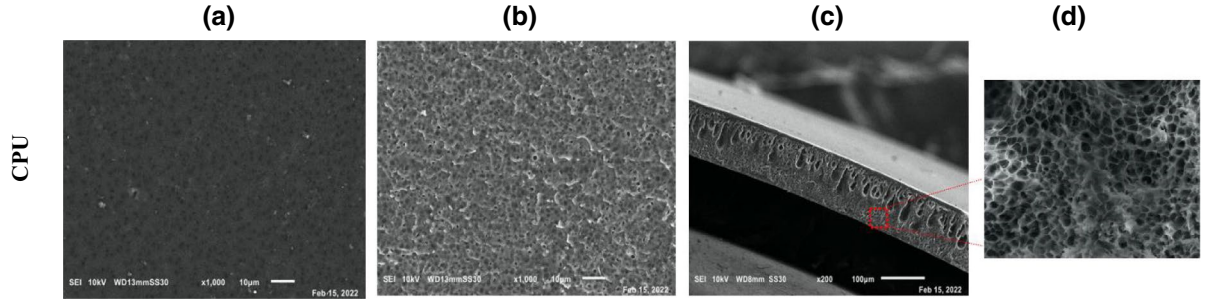

Fig. 6 SEM Images of **a** top **b** bottom and **c** cross section **d** sponge layer of CA/PVDF/UiO-66 membrane

distribution of UiO-66 NPs in the dope solution. The incorporated UiO-66 nanoparticles enhanced the permeability of water by providing an alternative path for the water molecules (Kim et al. 2019).

TGA was selected to express the membrane thermal decomposition by measuring the membrane weight change as a function of rising temperature. It is clearly indicated from Fig. 7 that each TGA curve

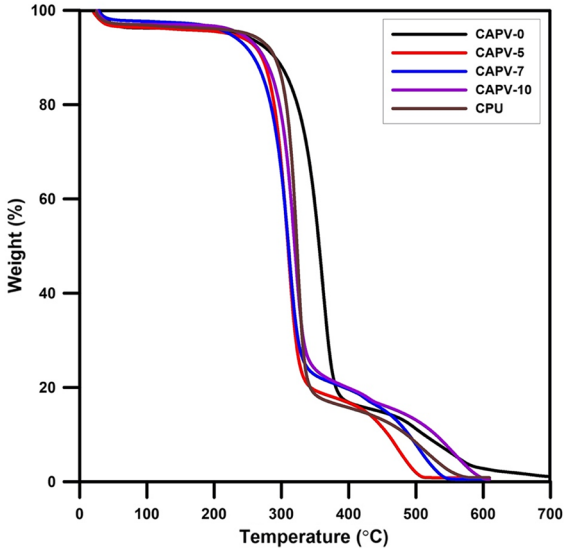

Fig. 7 TGA analysis of blank CA, blended CA/PVDF and hybrid CA/PVDF/UiO-66 membranes

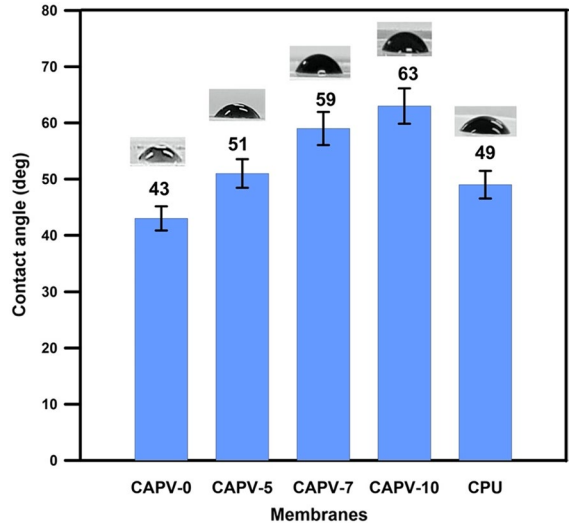

Fig. 8 Contact angle of the fabricated membranes

has 3 degradation steps. At the beginning, around 4% of the blank CA sample weight was lost because of evaporating any residual amounts of absorbed water and/or volatilizing existing volatile components by increasing the temperature from 30 to 230° C. Secondly, almost 84% of the original blank CA weight was decomposed due to the decomposition of cellulose acetate when escalating the temperature up to 400 °C. Similar results were previously reported in literature (De Campos et al. 2013). On the other hand, a slight enhancement in the thermal stability of pristine CA membrane was noticed with the addition of PVDF and UiO-66. It is clearly seen that, at 400 °C only 76.2 and 78% of CAPV-10 and CAPV-7 sample, respectively, was decomposed comparing to 84% of the CAPV-0. Moreover, the addition of UiO-66 nano-MOF to CA/PVDF blended polymeric membrane has further improvement of the membrane thermal stability. It was found that CPU membrane started to decompose at around 332 °C rather than 290 and 296 °C for CAPV-0 and CAPV-7, consecutively.

Contact angle was measured to evaluate the hydrophilicity of the various fabricated membranes. It gives an indication of the interaction between water and membrane surface. In general, when the measured contact angle (θ) is less than 90°, the membrane is considered hydrophilic. Consequently, the membrane is hydrophobic when its contact angle value is greater than 90°. It is also known that the value of θ has a reflection on the membrane surface roughness (Ba et al. 2019; Wu et al. 2020). As shown in Fig. 8, increasing the added amount of PVDF increased the value of contact angle from 43° to 63° (i.e., the membrane became more hydrophobic) in comparison to the pristine CA membrane. The findings showed that θ has increased from 43° for CAPV-0 to become 51° for CAPV-5. In addition, both CAPV-7 and CAPV-10 membranes showed the same trend, where θ value became 59° and 63°, respectively. However, the value of θ for all membranes was found to be below 90° (i.e., hydrophilic surfaces were still obtained after the PVDF addition). On the contrary, the impregnation of UiO-66 nanoparticles to CA/PVDF optimum membrane has decreased the value of θ to 49°.

Mechanical strength was tested to indicate the effect of PVDF and nanofiller addition into CA pristine membrane. The blending of PVDF with CA had an observable effect on the blank CA membrane mechanical stability. Figure 9 elaborates the improvement of mechanical strength with the increase of PVDF amounts. The mechanical stability of pure CA casted membrane is relatively low as it is considered a fragile polymer with a tensile strength equal to 2 MPa (Minhas et al. 2015; Asiri et al. 2022) compared with hard PVDF polymer that has 8.7 MPa tensile strength. Although, PVDF was added in small amounts with a maximum of 10 wt.%, it enhanced

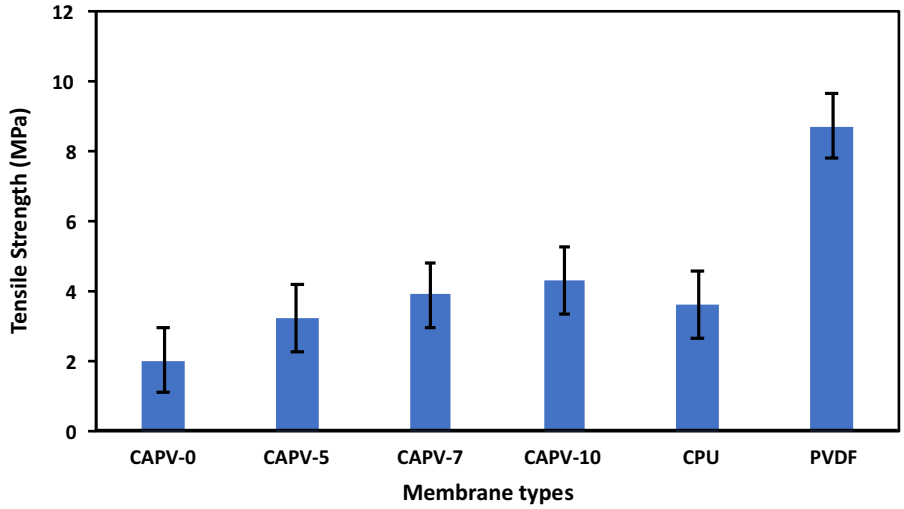

Fig. 9 Tensile strength of the fabricated membranes

the tensile strength of CA up to 4.3 MPa.This could be explained by the PVDF entrapment in CA polymeric matrix as it has higher mechanical strength compared to CA. Moreover, the reduction of macro voids with the addition of PVDF (Hossein Razzaghi et al. 2014) may improve the mechanical properties of blended membrane. This also confirms the successful blending of both CA and PVDF. On the other hand, the incorporation of UiO-66 NPs at 0.2 wt% with CA/PVDF (CAPV-7) blended membrane slightly decreased the tensile strength of the membrane from 3.8 MPa without UiO-66 to 3.6 MPa. This behavior could be returned to the presence of UiO-66 decreased the thickness of the sponge supportive layer. In addition, the incorporation of UiO-66 NPs at this selected amount might have caused a nanoparticles aggregation that weakened the mechanical properties of the hybrid membrane.

Blank CA, blended CA/PVDF and CA/PVDF/UiO-66 hybrid membranes performance evaluation

RO Performance of pristine CA, blended CA/PVDF and hybrid CA/PVDF/UiO-66 membranes

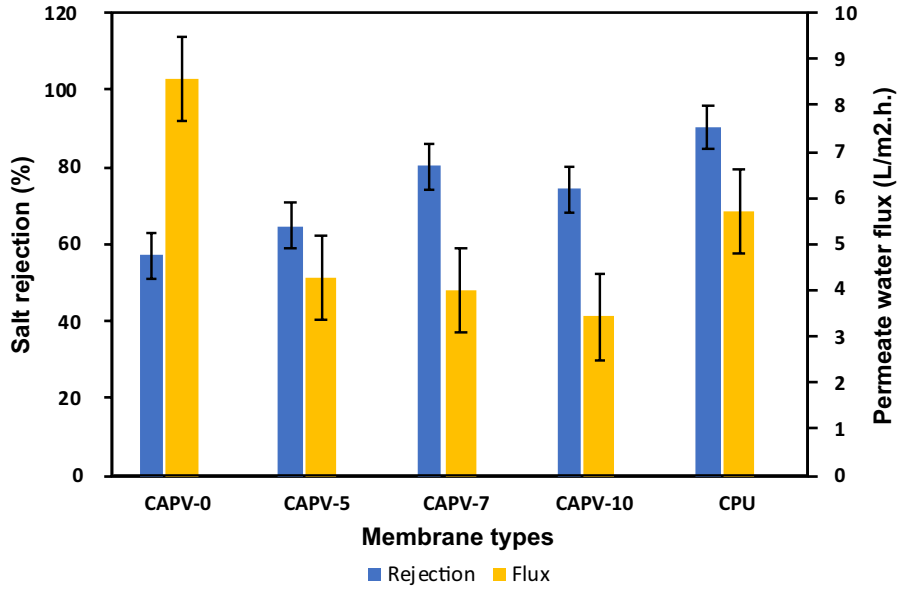

Fig. 10 A comparison between salt rejection and permeate water flux for the fabricated blank CA, blended CA/PVDF and hybrid CA/PVDF/UiO-66 membranes

was evaluated by calculating the membrane salt rejection and permeate water flux under a certain applied pressure. Figure 10 illustrates the comparison between permeate water flux and salt rejection for each membrane against the blank CA membrane at 8 bar. As it can be seen, blending PVDF with CA pristine membrane declined the permeate water flux along with a noticeable increase in the performance of salt rejection. Cellulose acetate (CA) is characterized by its hydrophilic nature while Polyvinylidene fluoride (PVDF) is known for its hydrophobic nature. Thus, the blending of two polymers contributed to reduce the membrane permeability as a result of decreasing the prepared membrane hydrophilicity. However, it was reported elsewhere that increasing the membrane surface hydrophobicity had a positive influence on enhancing the membrane salt rejection (Mansouri et al. 2018; Pang and Zhang 2018; Abdelhamid and Khalil 2019). Increasing the concentration of PVDF up to 7 wt% in the CA matrix resulted to a 40% enhancement of salt rejection and a 50% decline in permeate water flux. This might be explained as previously indicated at SEM images, that the addition of PVDF reduced the macrovoids in pristine CA membrane and escalated its small pores. However, increasing the concentration of PVDF above 7% led to a 7.5% decrease in salt rejection. This could be related to, above 7% PVDF a more viscous solution was obtained and in return a non-homogeneous membrane was obtained, and this had an effect on the membrane performance.

As a result, 7 wt% of PVDF was found to be the optimum weight and thus 0.2 wt%, relative to the total polymer weight, from UiO-66 nanoparticles were added to this membrane for further enhancement of its RO performance. It is clearly seen that the impregnation of UiO-66 nanoparticles increased the salt rejection and permeate water flux over CAPV-7 membrane by 12.5% and 42%, respectively. This can be explained as the incorporation of zirconium based UiO-66 nano filler increasing the membrane surface roughness and hydrophilicity (Trinh et al. 2021). Also, UiO-66 was previously found to have a small aperture window size (Cavka et al. 2008; Liu et al. 2019a), this size is greater than water molecules, which explains the increased water selectivity and as a result water permeability. Further, the increase in salt rejection percentage might be attributed to the smaller aperture size that UiO-66 has compared to Na^+ and Cl^- ions (Kadhom et al. 2017; Ma et al. 2017).

Conclusions

The aim of the presented work was to develop and obtain a new hybridized casted RO membrane. The aim was successfully acquired by the polymeric blending of CA with PVDF and the impregnation of MOF nanoparticles of previously prepared UiO-66. FTIR and XRD patterns proved the successful preparation and impregnation of the blended CA/PVDF polymeric membrane and mixed matrix membrane of CA/PVDF/UiO-66. The optimum mixing ratio of the two polymers was selected depending on the membrane with highest salt rejection percentage. Thus, CAPV-7 was found to be the optimum membrane with a salt rejection of 80.24% and a permeate water flux of 4 L/m2h. Then, 0.2 wt% nano MOF of the total polymer weight was impregnated to the CAPV-7 membrane to further improve its salt rejection and permeate water flux. Higher salt rejection and permeate water flux of 90.4% and 5.7 L/m2h, respectively, was established by the novel hybridized CPU membrane.

Acknowledgments The authors would like to thank the Science, Technology & innovation Funding Authority (STDF) and Egyptian Knowledge Bank EKB for fundingand facilitating the procedures for publishing this work.

Author contributions Conceptualization, OAK, MFE, AHE MSS; methodology, OAK; validation, OAK, MFE and MSS; formal analysis, OAK and MFE; investigation, OAK and MFE; resources, MFE, AHE and MSS; visualization, OAK; writing-original draft preparation, OAK; writing-review and editing, OAK, AHE, MSS and MFE; supervision, MSS, AHE and MFE. All authors have read and agreed to the published version of the manuscript.

Funding Open access funding provided by The Science, Technology & Innovation Funding Authority (STDF) in cooperation with The Egyptian Knowledge Bank (EKB). The authors declare that no funds, grants, or other support were received during the preparation of this manuscript.

Declarations

Conflict of interest The authors have no relevant financial or non-financial interests to disclose.

References

Abdelhamid AE, Khalil AM (2019) Polymeric membranes based on cellulose acetate loaded with candle soot nanoparticles for water desalination. J Macromol Sci Part A 56:153–161. https://doi.org/10.1080/10601325.2018.1559698

Abdellah Ali SF, William LA, Fadl EA (2020) Cellulose acetate, cellulose acetate propionate and cellulose acetate butyrate membranes for water desalination applications. Cellulose 27:9525–9543. https://doi.org/10.1007/s10570-020-03434-w

Ahmad A, Waheed S, Khan SM et al (2015) Effect of silica on the properties of cellulose acetate/polyethylene glycol membranes for reverse osmosis. Desalination 355:1–10. https://doi.org/10.1016/j.desal.2014.10.004

Ahmed MK, El-Naggar ME, Mahmoud KH et al (2021) Electrospun membranes of cellulose acetate/polyvinylidene difluoride containing Au/Se nanoparticles via laser ablation technique for methylene blue degradation. J Polym Res 28:1–9. https://doi.org/10.1007/s10965-021-02680-1

Aldalbahi A, El-naggar M, Khattab T et al (2020) Development of green and sustainable cellulose acetate/graphene oxide nanocomposite films as efficient adsorbents for wastewater treatment. Polymers (basel) 12:1–16. https://doi.org/10.3390/polym12112501

Ali ASM, Soliman MM, Kandil SH, Khalil MMA (2021) Emerging mixed matrix membranes based on zeolite nanoparticles and cellulose acetate for water desalination. Cellulose 28:6417–6426. https://doi.org/10.1007/s10570-021-03924-5

Arthanareeswaran G, Kumar SA (2010) Effect of additives concentration on performance of cellulose acetate and polyethersulfone blend membranes. J Porous Mater 17:515–522. https://doi.org/10.1007/s10934-009-9319-y

Asiri AM, Pugliese V, Petrosino F et al (2022) Photocatalytic degradation of textile dye on blended cellulose acetate membranes. Polymers (basel). https://doi.org/10.3390/polym14030636

Ba X, Wang X, Cui N et al (2019) Preparation, characterisation, and desalination performance study of cellulose acetate membranes with MIL-53(Fe) additive. J Memb Sci. https://doi.org/10.1016/j.memsci.2019.04.061

Batool M, Shafeeq A, Haider B, Ahmad NM (2021) TiO_2 nanoparticle filler-based mixed-matrix PES/CA nanofiltration membranes for enhanced desalination. Membranes 11:433. https://doi.org/10.3390/membranes11060433

Cavka JH, Jakobsen S, Olsbye U et al (2008) A new zirconium inorganic building brick forming metal organic frameworks with exceptional stability. J Am Chem Soc 130:13850–13851. https://doi.org/10.1021/ja8057953

Cui J, Liu J, He C et al (2017) Composite of polyvinylidene fluoride–cellulose acetate with $Al(OH)_3$ as a separator for high-performance lithium ion battery. J Memb Sci 541:661–667. https://doi.org/10.1016/j.memsci.2017.07.048

Da Silva PB, Moreti LOR, Silva MF et al (2017) Water permeability increase in ultrafiltration cellulose acetate membrane containing silver nanoparticles. Mater Res 20:887–891. https://doi.org/10.1590/1980-5373-MR-2016-1074

De Campos EA, De Campos SD, Roos AA et al (2013) Titanium dioxide dispersed on cellulose acetate and its application in methylene blue photodegradation. Polym Polym Compos 21:423–430. https://doi.org/10.1177/096739111302100703

Duarte AP, Cidade MT, Bordado JC (2006) Cellulose acetate reverse osmosis membranes: optimization of the composition. J Appl Polym Sci 100:4052–4058. https://doi.org/10.1002/app.23237

El-Aassar MR, El-Kady MF, Hassan HS, Al-Deyab SS (2016) Synthesis and characterization of surface modified electrospun poly (acrylonitrile-co-styrene) nanofibers for dye decolorization. J Taiwan Inst Chem Eng 58:274–282. https://doi.org/10.1016/j.jtice.2015.05.042

Elessawy NA, El-Sayed EM, Ali S et al (2020) One-pot green synthesis of magnetic fullerene nanocomposite for adsorption characteristics. J Water Process Eng 34:101047. https://doi.org/10.1016/j.jwpe.2019.101047

El-Gendi A, Abdallah H, Amin A, Amin SK (2017) Investigation of polyvinylchloride and cellulose acetate blend membranes for desalination. J Mol Struct 1146:14–22. https://doi.org/10.1016/j.molstruc.2017.05.122

El-Ghaffar MAA, Elawady MM, Rabie AM, Abdelhamid AE (2020) Enhancing the RO performance of cellulose acetate membrane using chitosan nanoparticles. J Polym Res 27:1–12. https://doi.org/10.1007/s10965-020-02319-7

Elkady M, Shokry H, Hamad H (2020) New activated carbon from mine coal for adsorption of dye in simulated water or multiple heavy metals in real wastewater. Materials (basel). https://doi.org/10.3390/ma13112498

Elkony Y, Mansour ES, Elhusseiny A et al (2020) Novel grafted/crosslinked cellulose acetate membrane with N-isopropylacrylamide/N, N-methylenebisacrylamide for water desalination. Sci Rep 10:1–13. https://doi.org/10.1038/s41598-020-67008-3

Fitri SJ, Widiastuti N (2017) Preparation of polyvinylidene fluoride/cellulose acetate blend membrane with polyethylene glycol additive for apple juice clarification. In: AIP Conference Proceedings. https://doi.org/10.1063/1.4978164

Ghaffarian V, Mousavi SM, Bahreini M, Afifi M (2013) Preparation and characterization of biodegradable blend membranes of PBS/CA. J Polym Environ 21:1150–1157. https://doi.org/10.1007/s10924-012-0551-1

Ghaseminezhad SM, Barikani M, Salehirad M (2019) Development of graphene oxide-cellulose acetate nanocomposite reverse osmosis membrane for seawater desalination. Compos Part B Eng 161:320–327. https://doi.org/10.1016/j.compositesb.2018.10.079

Haponska M, Trojanowska A, Nogalska A et al (2017) PVDF membrane morphology—influence of polymer molecularweight and preparation temperature. Polymers (basel) 9:1–14. https://doi.org/10.3390/polym9120718

He Y, Tang YP, Ma D, Chung TS (2017) UiO-66 incorporated thin-film nanocomposite membranes for efficient selenium and arsenic removal. J Memb Sci 541:262–270. https://doi.org/10.1016/j.memsci.2017.06.061

Hołda AK, Vankelecom IFJ (2015) Understanding and guiding the phase inversion process for synthesis of solvent resistant nanofiltration membranes. J Appl Polym Sci 132:1–17. https://doi.org/10.1002/app.42130

Hossein Razzaghi M, Safekordi A, Tavakolmoghadam M et al (2014) Morphological and separation performance study of PVDF/CA blend membranes. J Memb Sci 470:547–557. https://doi.org/10.1016/j.memsci.2014.07.026

Kadhom M, Hu W, Deng B (2017) Thin film nanocomposite membrane filled with metal-organic frameworks UiO-66 and MIL-125 nanoparticles for water desalination. Membranes (basel). https://doi.org/10.3390/membranes7020031

Kamal H, Abd-Elrahim FM, Lotfy S (2014) Characterization and some properties of cellulose acetate-co-polyethylene oxide blends prepared by the use of gamma irradiation. J Radiat Res Appl Sci 7:146–153. https://doi.org/10.1016/j.jrras.2014.01.003

Kang W, Ma X, Zhao H et al (2016) Electrospun cellulose acetate/poly(vinylidene fluoride) nanofibrous membrane for polymer lithium-ion batteries. J Solid State Electrochem 20:2791–2803. https://doi.org/10.1007/s10008-016-3271-y

Kim T, Choi MK, Ahn HS et al (2019) Fabrication and characterization of zeolitic imidazolate framework-embedded cellulose acetate membranes for osmotically driven membrane process. Sci Rep 9:1–10. https://doi.org/10.1038/s41598-019-42235-5

Koriem OA, El-Shazly AH, El-Kady MF (2021) A study of the effect of reaction time on the preparation of zirconium based UiO-66 MOF. Key Eng Mater 897:57–62. https://doi.org/10.4028/www.scientific.net/kem.897.57

Li M, Katsouras I, Piliego C et al (2013) Controlling the microstructure of poly(vinylidene-fluoride) (PVDF) thin films for microelectronics. J Mater Chem C 1:7695–7702. https://doi.org/10.1039/c3tc31774a

Liu C, Bai R (2005) Preparation of chitosan/cellulose acetate blend hollow fibers for adsorptive performance. J Memb Sci 267:68–77. https://doi.org/10.1016/j.memsci.2005.06.001

Liu L, Xie X, Qi S, Li R, Zhang X, Song X, Gao C (2019) Thin film nanocomposite reverse osmosis membrane incorporated with UiO-66 nanoparticles for enhanced boron removal. J Memb Sci 580:101–109. https://doi.org/10.1016/j.memsci.2019.02.072

Liu S, Hu LF, Zhang WC, Ma HY (2019b) Cellulose acetate reverse osmosis membranes for desalination: a short review. Non Met Mater Sci 1:14–24. https://doi.org/10.30564/omms.v1i2.1143

Lu Y, Ma Y, Yang T, Guo J (2021) Hydrophilic modification of PVDF membranes by in situ synthesis of nano-Ag with nano-ZrO_2. Green Process Synth 10:538–546. https://doi.org/10.1515/gps-2021-0050

Ma D, Peh SB, Han G, Chen SB (2017) Thin-film nanocomposite (TFN) membranes incorporated with super-hydrophilic metal-organic framework (MOF) UiO-66: toward enhancement of water flux and salt rejection. ACS Appl Mater Interfaces 9:7523–7534. https://doi.org/10.1021/acsami.6b14223

Mansouri S, Khalili S, Peyravi M et al (2018) Sublayer assisted by hydrophilic and hydrophobic ZnO nanoparticles toward engineered osmosis process. Korean J Chem Eng 35:2256–2268. https://doi.org/10.1007/s11814-018-0086-9

Minhas FT, Farrukh S, Hussain A, Mujahid M (2015) Comparison of silica and novel functionalized silica-based cellulose acetate hybrid membranes in gas permeation study. J Polym Res 22:1–13. https://doi.org/10.1007/s10965-015-0701-y

Moradihamedani P, Abdullah AH (2017) High-performance cellulose acetate/polysulfone blend ultrafiltration membranes for removal of heavy metals from water. Water Sci Technol 75:2422–2433. https://doi.org/10.2166/wst.2017.122

Morsy A, Ebrahim S, Kenawy ER et al (2016) Grafted cellulose acetate reverse osmosis membrane using 2-acrylamido-2-methylpropanesulfonic acid for water desalination. Water Sci Technol Water Supply 16:1046–1056. https://doi.org/10.2166/ws.2016.025

Nagendran A, Arockiasamy DL, Mohan D (2008) Cellulose acetate and polyetherimide blend ultrafiltration membranes, i: preparation, characterization, and application. Mater Manuf Process 23:311–319. https://doi.org/10.1080/10426910801974812

Ning ATAEEE-RY (2015) Phase diagram and membrane desalination. IntechOpen, Rijeka, p 3

Ounifi I, Guesmi Y, Ursino C et al (2021) Antifouling membranes based on cellulose acetate (CA) blended with poly(acrylic acid) for heavy metal remediation. Appl Sci. https://doi.org/10.3390/app11104354

Pang R, Zhang K (2018) Fabrication of hydrophobic fluorinated silica-polyamide thin film nanocomposite reverse osmosis membranes with dramatically improved salt rejection. J Colloid Interface Sci 510:127–132. https://doi.org/10.1016/j.jcis.2017.09.062

Rana D, Matsuura T, Kassim M, Ismail A (2015) Reverse osmosis membrane. Handb Membr Se. https://doi.org/10.1201/b18319-5

Razzaghi MH, Tavakolmoghadam M, Rekabdar F, Oveisi F (2018) Investigation of the effect of coagulation bath composition on PVDF/CA membrane by evaluating critical flux and antifouling properties in lab-scale submerged MBR. Water Environ J 32:366–376. https://doi.org/10.1111/wej.12334

Reza M, Promono E, Radiman CL (2022) Improving separation performance of PVDF ultrafiltration membranes by blending with cellulose acetate. Iran J Chem Chem Eng. https://doi.org/10.30492/ijcce.2022.550394.5221

Salameh MTB, Alraggad M, Harahsheh ST (2021) The water crisis and the conflict in the Middle East. Sustain Water Resour Manag 7:69. https://doi.org/10.1007/s40899-021-00549-1

Schelling M, Kim M, Otal E, Hinestroza J (2018) Decoration of cotton fibers with a water-stable metal–organic framework (UiO-66) for the decomposition and enhanced adsorption of micropollutants in water. Bioengineering. https://doi.org/10.3390/bioengineering5010014

Shah V, Wang B, Li K (2021) High-performance PVDF membranes prepared by the combined crystallisation and diffusion (CCD) method using a dual-casting technique: a breakthrough for water treatment applications. Energy Environ Sci 14:5491–5500. https://doi.org/10.1039/d1ee02009a

Sharma SK, Verma DS, Khan LU et al (2018) Handbook of materials characterization. Handb Mater Charact. https://doi.org/10.1007/978-3-319-92955-2

Siddique T, Dutta NK, Choudhury NR (2021) Mixed-matrix membrane fabrication for water treatment. Membranes (basel). https://doi.org/10.3390/membranes11080557

Sivakumar M, Mohan DR, Rangarajan R (2006) Studies on cellulose acetate-polysulfone ultrafiltration membranes: ii. Effect of additive concentration. J Memb Sci 268:208–219. https://doi.org/10.1016/j.memsci.2005.06.017

Strathmann H, Scheible P, Baker RW (1971) A rationale for the preparation of Loeb-Sourirajan-type cellulose acetate membranes. J Appl Polym Sci 15:811–828. https://doi.org/10.1002/app.1971.070150404

Struzyńska-Piron I, Bilad MR, Loccufier J et al (2014) Influence of UV curing on morphology and performance of polysulfone membranes containing acrylates. J Memb Sci 462:17–27. https://doi.org/10.1016/j.memsci.2014.03.013

Nunes SP, Peinemann KV (2006) Chemie.ir. Wiley-VCH Gmbh & Co. KGaA, Weinheim

Trinh DX, Pham NN, Chammingkwan P, Taniike T (2021) Preparation and desalination performance of PA/UiO-66/PES composite membranes. Membranes (basel) 11:2–11. https://doi.org/10.3390/membranes11080628

Werber J, Osuji C, Elimelech M (2016) Materials for next-generation desalination and water purification membranes. Nat Rev Mater 1. https://doi.org/10.1038/natrevmats.2016.18

Wu B, Wang S, Wang J et al (2020) Facile fabrication of high-performance thin film nanocomposite desalination membranes imbedded with alkyl group-capped silica nanoparticles. Polymers (basel). https://doi.org/10.3390/polym12061415

Xu F, Weng B, Materon LA et al (2016) Fabrication of cellulose fine fiber based membranes embedded with silver nanoparticles via Forcespinning. J Polym Eng 36:269–278. https://doi.org/10.1515/polyeng-2015-0092

Zhang Q, Yang T, Liu X et al (2019) Heteropoly acid-encapsulated metal-organic framework as a stable and highly efficient nanocatalyst for esterification reaction. RSC Adv 9:16357–16365. https://doi.org/10.1039/c9ra03209f

Zhao S, Liao Z, Fane A et al (2021) Engineering antifouling reverse osmosis membranes: A review. Desalination 499:114857. https://doi.org/10.1016/j.desal.2020.114857